A Dual-Band Coupled-Line Coupler With an Arbitrary Coupling Coefficient

Xi Wang, Wen-Yan Yin, *Senior Member, IEEE*, and Ke-Li Wu, *Fellow, IEEE*

***Abstract*—A novel dual-band coupled-line coupler with an arbitrary coupling coefficient is proposed and investigated in this paper. The coupler has a simple structure and can realize a wide range of the same coupling coefficient over two designated frequencies. The mathematical design formula is also developed, which not only provides a straightforward design procedure, but also reveals the attractive features of the proposed coupler, including: 1) the same coupling coefficient in the dual frequency bands; 2) the sole dependence of a coupling coefficient on the ratio of the impedances of even and odd modes; and 3) a large range of the ratio of the dual frequencies. Two prototypes of the proposed couplers, one operating at 2.4/5.8 GHz with a −10-dB coupling coefficient and the other working at 0.9/1.8 GHz with a −15-dB coupling coefficient, have been designed, fabricated, and measured. The measured results demonstrate that the bandwidths for the 2.4- and 5.8-GHz bands are 22% and 19.8%, respectively, and that for the 0.9- and 1.8-GHz bands are 28.4% and 15.8%, respectively. Good correlation between the measured results and those of the theoretically designed justifies the proposed coupler circuit and the design theory.**

***Index Terms*—Arbitrary coupling coefficient, coupled-line coupler, dual band.**

I. Introduction

WITH THE increasing demands on coexistence of multiple wireless communication systems in one outdoor unit, such as global system for mobile communications (GSM), Universal Mobile Telecommunications System (UMTS), and future long-term evolution (LTE) systems, more and more dual-band or even multiple-band RF and microwave subsystems are required for sharing the resources, reducing system complicity, and cutting down the cost as much as possible. To this end, much research has been devoted to various dual-band RF passive components, such as dual-band antennas [1], [2], filters [3], [4], power dividers [5], [6], and branch-line couplers [7]–[14].

Regarding dual-band couplers, a lot of attention has been paid to a dual-band branch-line coupler, which can be used in balanced amplifiers, mixers, phase shifters, and antenna arrays. For example, a branch-line dual-band coupler using left-handed transmission lines was proposed in 2003 [7]. In [8], additional open- or short-circuit stubs tapped to the end of each branch line were introduced for designing a dual-band branch-line coupler with simple and analytical design equations. A stub tapped to the center of each branch line [9], [10] can also realize a dual-band coupler. Cross branches, which can provide additional freedom, were utilized to design dual-band couplers in [11]. In [12], a novel 3-dB dual-band branch-line coupler was introduced with a simple port extension.

All of the above-mentioned research was based on branch-line couplers or rat-race couplers with a −3-dB coupling coefficient. In practice, different coupling coefficients are required for different system requirements. For example, a small amount of signal needs to be coupled to a monitoring circuit at an antenna feeding port. In this direction, a dual-band branch-line coupler and a rat-race coupler with arbitrary couplings were proposed [13] with limited coupling coefficients due to a limited realizable high-impedance value. For example, the characteristic impedance of the shunt branch lines needs to be 500 Ω to realize a −20-dB coupling coefficient. To decrease the coupling, [14] used a coupled line instead of a transmission line in a branch-line coupler. In this study, the bandwidths of the sample coupler are only 8.1% and 1.91% at the two designated frequencies, respectively. Most recently, a 3-dB dual-band coupled-line coupler has been proposed in [15], which is relatively compact and requires a relatively smaller footprint to implement as compared to a branch-line coupler.

In this paper, a dual-band coupled-line coupler with an arbitrary coupling coefficient and a large range of frequency ratios is proposed. The coupler configuration consists of three pairs of coupled lines with the same coupling coefficient in the dual frequencies. It has a wider bandwidth than that of a branch-line coupler and a greater flexibility in controlling the coupling coefficient. The proposed coupler can be easily realized by a double-sided printed circuit board (PCB). One of the attractive attributes that is worthwhile to mention is, similar to a conventional coupled-line coupler, a different coupling coefficient can be realized by controlling the ratio of the impedances of even and odd modes of the coupled lines. Additionally, the phase difference between the two output ports almost remains a constant 90° in a very wideband range.

Manuscript received October 15, 2011; revised January 08, 2012; accepted January 10, 2012. Date of publication February 20, 2012; date of current version April 04, 2012.This work was supported by the Research Grants Council of the Hong Kong Special Administrative Region under Grant 2150647. This work was supported in part by the National Basic Research Program of China under Grant 2009CB320204.

X. Wang is with the Department of Electronic Engineering, The Chinese University of Hong Kong, Shatin, Hong Kong, and also with the School of Electronic Information and Electrical Engineering, Shanghai Jiao Tong University, Shanghai 200240, China (e-mail: xwang@ee.cuhk.edu.hk).

W.-Y. Yin is with the Center for Microwave and RF Technologies, Shanghai Jiao Tong University, Shanghai 200240, China, and also with the Center for Optical and Electromagnetic Research, State Key Laboraotory of Modern Optical Instrumentation, Zhejiang University, Hangzhou 310058, China (e-mail: wyyin@sjtu.edu.cn; wyyin@zju.edu.cn).

K.-L. Wu is with the Department of Electronic Engineering, The Chinese University of Hong Kong, Shatin, Hong Kong (e-mail: klwu@ee.cuhk.edu.hk).

Color versions of one or more of the figures in this paper are available online at http://ieeexplore.ieee.org.

Digital Object Identifier 10.1109/TMTT.2012.2185949

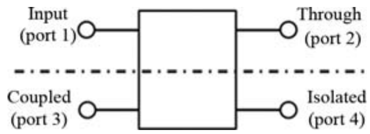

Fig. 1. Schematic diagram of a symmetrical coupler network.

This paper is organized as follows. In Section II, the matching and isolation conditions of a symmetrical four-port network is analyzed first, which is the foundation for designing a coupled-line coupler. The configuration of the proposed dual-band coupler and its design theory are then introduced, followed by the discussion on the achievable frequency ratios based on a realizable impedance of the coupled line using an ordinary PCB fabrication process. Section III shows the simulated and measured results of two prototypes of the proposed dual-band coupler with different coupling coefficients and different frequency ratios, of which one operates at 2.4/5.8 GHz with -10-dB coupling coefficient, and the other operates at 0.9/1.8 GHz with -15-dB coupling coefficient. The measured results agree well with the simulated ones.

II. Theory

A. Matching and Isolation Conditions

For a general coupled-line coupler, as shown in Fig. 1, the S-parameters can be expressed in terms of its corresponding even- and odd-mode half-circuits by

$$S_{11} = \frac{1}{2}(S_{11e} + S_{11o}) = 0 \tag{1a}$$
$$S_{21} = \frac{1}{2}(S_{21e} + S_{21o}) = -j\sqrt{1-C^2} \tag{1b}$$
$$S_{31} = \frac{1}{2}(S_{11e} - S_{11o}) = C \tag{1c}$$
$$S_{41} = \frac{1}{2}(S_{21e} - S_{21o}) = 0 \tag{1d}$$

where

$$S_{11e} = \frac{A_e + \frac{B_e}{Z_0} - C_e \cdot Z_0 - D_e}{A_e + \frac{B_e}{Z_0} + C_e \cdot Z_0 + D_e} \tag{2a}$$
$$S_{21e} = \frac{2}{A_e + \frac{B_e}{Z_0} + C_e \cdot Z_0 + D_e} \tag{2b}$$
$$S_{11o} = \frac{A_o + \frac{B_o}{Z_0} - C_o \cdot Z_0 - D_o}{A_o + \frac{B_o}{Z_0} + C_o \cdot Z_0 + D_o} \tag{2c}$$
$$S_{21o} = \frac{2}{A_o + \frac{B_o}{Z_0} + C_o \cdot Z_0 + D_o} \tag{2d}$$

and C is the coupling of the coupler, As, Bs, Cs, and Ds, where $s = e$ and o are the elements of $[A, B, C, D]$ matrices of even- and odd-mode half-circuits, respectively.

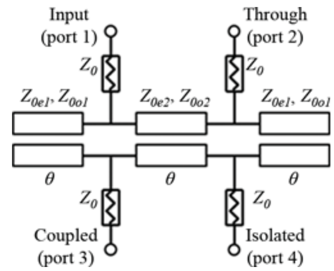

Fig. 2. Schematic diagram of the proposed dual-band coupler.

For a reciprocal and lossless two-port network, $A_{e,o}$ and $D_{e,o}$ are pure real, and $B_{e,o}$ and $C_{e,o}$ are pure imaginary. Clearly, (1d) leads to

$$A_e + D_e = A_o + D_o \tag{3a}$$
$$\frac{B_e}{Z_0} + C_e \cdot Z_0 = \frac{B_o}{Z_0} + C_o \cdot Z_0. \tag{3b}$$

To satisfy (1a), one can find that

$$\frac{B_e}{Z_0} - C_e \cdot Z_0 + \left(\frac{B_o}{Z_0} - C_o \cdot Z_0\right) = 0. \tag{4}$$

Equations (3b) and (4) can be rewritten as

$$\frac{B_e}{Z_0} = C_o \cdot Z_0 \tag{5a}$$
$$\frac{B_o}{Z_0} = C_e \cdot Z_0. \tag{5b}$$

Equations (3a) and (5) are the simultaneous matching and isolation conditions of a symmetric four-port coupler network.

B. Proposed Coupler Circuit and Its Design Formula

The schematic diagram of the proposed dual-band coupled-line coupler is shown in Fig. 2 with port terminated by the impedance of Z_0. The coupler consists of three pairs of coupled lines with the same electrical length θ. The coupled lines on the two sides are assumed to be identical. The corresponding even- and odd-mode half-circuits of the coupler are presented in Fig. 3 in terms of even- and odd-mode characteristic impedances Z_{0e1}, Z_{0o1}, Z_{0e2}, and Z_{0o2} of coupled line Sections I and II, respectively. The elements of $[A, B, C, D]$ matrices for even- and odd-mode half-circuits can be found as

$$A_e = D_e = \cos\theta - \frac{Z_{0e2}\sin^2\theta}{Z_{0e1}\cos\theta} \tag{6a}$$
$$B_e = jZ_{0e2}\sin\theta \tag{6b}$$
$$C_e = j\frac{2\sin\theta}{Z_{0e1}} + j\frac{\sin\theta}{Z_{0e2}} - j\frac{Z_{0e2}\sin^3\theta}{Z_{0e1}^2\cos^2\theta} \tag{6c}$$
$$A_o = D_o = \cos\theta - \frac{Z_{0o2}\sin^2\theta}{Z_{0o1}\cos\theta} \tag{7a}$$
$$B_o = jZ_{0o2}\sin\theta \tag{7b}$$
$$C_o = j\frac{2\sin\theta}{Z_{0o1}} + j\frac{\sin\theta}{Z_{0o2}} - j\frac{Z_{0o2}\sin^3\theta}{Z_{0o1}^2\cos^2\theta}. \tag{7c}$$

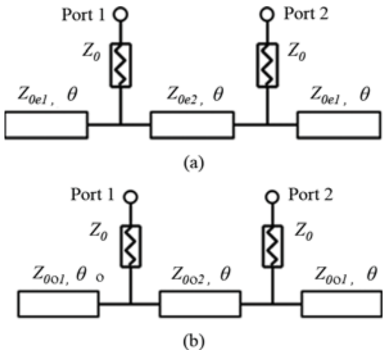

Fig. 3. Even- and odd-mode half-circuits. (a) Even mode. (b) Odd mode.

As expected, $A_{e,o}$ and $D_{e,o}$ are pure real, and $B_{e,o}$ and $C_{e,o}$ are pure imaginary. From the matching and isolation conditions (3a) and (5), the following equations can be obtained:

$$\frac{Z_{0e1}}{Z_{0e2}} = \frac{Z_{0o1}}{Z_{0o2}} = k \tag{8}$$

$$\frac{Z_{0e2}Z_{0o2}}{Z_0^2} = \frac{2}{k} + 1 - \frac{\tan^2\theta}{k^2}. \tag{9}$$

Since the dependence of θ in (9) is governed by function $\tan^2\theta$, for any values of Z_{0e1}, Z_{0o1}, Z_{0e2}, Z_{0o2}, and Z_0, there are two solutions for variable θ in each π cycle. If θ_1 and θ_2 are the first two solutions of (9) and f_1 and f_2 are the corresponding frequencies. For a quasi-dispersion-free coupled line, there are

$$\theta_1 = \pi - \theta_2 \tag{10a}$$

$$\frac{f_2}{f_1} = \frac{\theta_2}{\theta_1} \tag{10b}$$

or

$$\theta_1 = \frac{\pi}{1 + \dfrac{f_2}{f_1}}. \tag{10c}$$

Obviously, two conclusions can be drawn at this point, which are: 1) for a given set of values of Z_{0e1}, Z_{0o1}, Z_{0e2}, Z_{0o2}, and Z_0, the two operating frequencies f_1 and f_2 are uniquely determined and 2) at the arithmetic average frequency of f_1 and f_2, the electrical length θ equals to $\pi/2$. These two conclusions set the basic design rule of how to control the dual frequencies of the proposed coupler.

Furthermore, with the help of (3a) and (5), parameters of S_{21} and S_{31} of the coupler can be expressed as

$$S_{21} = \frac{2}{2\left(\cos\theta - \dfrac{Z_{0e2}\sin^2\theta}{Z_{0e1}\cos\theta}\right) + j\dfrac{(Z_{0e2}+Z_{0o2})\sin\theta}{Z_0}} \tag{11}$$

$$S_{31} = \frac{j\dfrac{(Z_{0e2}-Z_{0o2})\sin\theta}{Z_0}}{2\left(\cos\theta - \dfrac{Z_{0e2}\sin^2\theta}{Z_{0e1}\cos\theta}\right) + j\dfrac{(Z_{0e2}+Z_{0o2})\sin\theta}{Z_0}}. \tag{12}$$

It can be proven that if

$$Z_{0e2}Z_{0o2} = \frac{Z_0^2}{\sin^2\theta} \tag{13}$$

then (9) becomes

$$k = \tan^2\theta. \tag{14}$$

By defining a new parameter C' such that

$$C' = \frac{\dfrac{Z_{0e2}}{Z_{0o2}} - 1}{\dfrac{Z_{0e2}}{Z_{0o2}} + 1} = \frac{\dfrac{Z_{0e1}}{Z_{0o1}} - 1}{\dfrac{Z_{0e1}}{Z_{0o1}} + 1} \tag{15}$$

for where the matching and isolation condition (8) has been employed, S_{21} and S_{31} of the proposed dual-band coupler are reduced to

$$S_{21} = -j\sqrt{1 - C'^2} \tag{16a}$$

$$S_{31} = C'. \tag{16b}$$

Equation (16) justifies that parameter C' is the coupling coefficient of the coupler. In other words, the proposed dual-band coupled-line coupler satisfies the same electric properties at its dual operating frequencies as those of the conventional single-band coupled-line coupler. Having revealed by (16), the parameter C' represents the coupling of the proposed coupler and is determined by the ratio Z_{0e}/Z_{0o} only. The larger the ratio is, the larger coupling coefficient can be achieved.

The design procedure of the coupler can be summarized as follows.

1) For given two designated frequencies, using (10) to determine θ, $\sin\theta$ and $\tan\theta$, where $\theta = \theta_1$ or θ_2.
2) For a required coupling coefficient C', Z_{0e2} and Z_{0o2} can be obtained using (13) and (15), or more specifically

$$Z_{0e2} = \frac{Z_0\sqrt{\dfrac{1+C'}{1-C'}}}{\sin\theta} \tag{17a}$$

$$Z_{0o2} = \frac{Z_0\sqrt{\dfrac{1-C'}{1+C'}}}{\sin\theta}. \tag{17b}$$

3) Z_{0e1} and Z_{0o1} are determined by (8) and (14).

For a practical application, the required coupled transmission lines must be realizable. An equivalent characteristic impedance of a pair of edge-coupled microstrip coupled lines that is approximately equal to the characteristic impedance of the half-circuit of the even or odd mode of the coupled line when the coupling is very weak can be defined by

$$Z_{\text{eq}} = \sqrt{Z_{0e} \cdot Z_{0o}}. \tag{18}$$

It can be seen from (17) and (18) that $Z_{\text{eq}1}$ and $Z_{\text{eq}2}$, the equivalent characteristic impedances for coupled line Sections I and II, respectively, are a constant if the dual operating frequencies are given. Since $Z_{\text{eq}1}$ and $Z_{\text{eq}2}$ are only the functions of θ, if the termination Z_0 is given, the limitation of a realizable

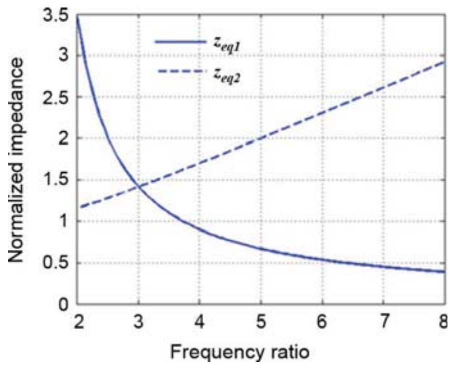

Fig. 4. Normalized equivalent characteristic impedances of coupled-line sections 1 and 2 versus frequency ratio.

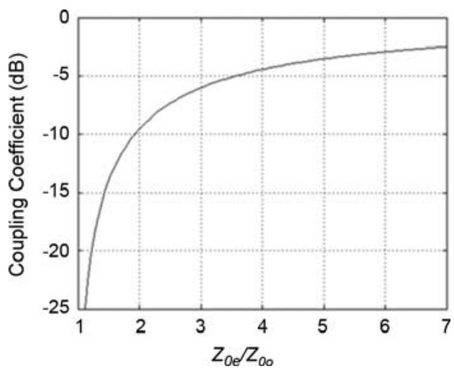

Fig. 5. Coupling coefficient of the proposed coupler versus the ratio of Z_{0e}/Z_{0o}.

coupled line mainly depends on the separation of the dual frequencies. Fig. 4 shows the normalized equivalent characteristic impedances of $Z_{\mathrm{eq}1}$ and $Z_{\mathrm{eq}2}$ to Z_0 versus frequency ratio of the dual frequencies. It can be observed that equivalent characteristic impedances of $Z_{\mathrm{eq}1}$ and $Z_{\mathrm{eq}2}$ can be easily realized in a wide range of frequency ratios.

Fig. 5 shows the coupling coefficient versus the impedance ratio of Z_{0e}/Z_{0o}. Theoretically speaking, to realize a -3-dB coupler, the ratio needs to be 5.83, which is not easy to achieve by a double-sided PCB board. Some auxiliary approaches can be applied to increase the coupling of a coupled line, e.g., a pair of coupled line with an aperture opened on the ground plane was proposed to achieve a large ratio of Z_{0e}/Z_{0o} by a double-sided PCB [16]. Therefore, the proposed coupled-line coupler can realize an arbitrary coupling coefficient using a double-sided PCB board.

III. Design Examples

Unlike a branch-line coupler, the phase difference of a coupled-line coupler remains constant in and out of the operating frequency band. This property is retained in the proposed dual-band coupled-line coupler. Fig. 6 shows the theoretic responses of ideal proposed dual-band coupled-line couplers with coupling coefficients of -3, -10, and -20 dB at dual operating frequencies of 1 and 3 GHz. The electrical parameters of the circuit model can be found by using (10), (17), and (18) with Z_0 set to 50 Ω. The 1-dB ripple is set in defining the bandwidth. For the -3-dB coupler design, the designed parameters

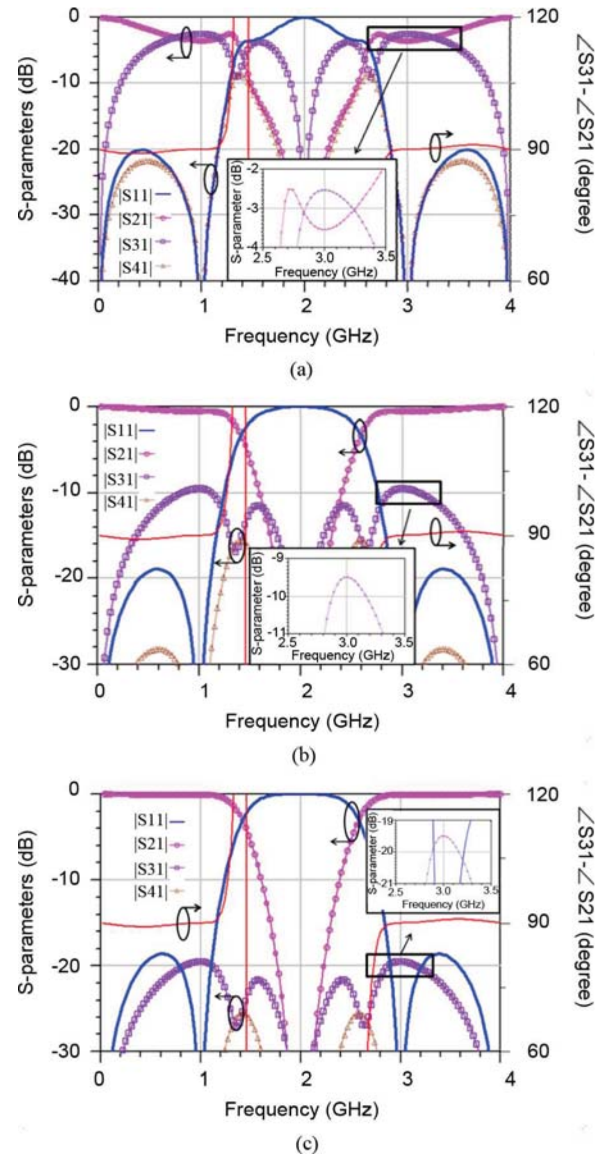

Fig. 6. Frequency response and phase difference of ideal circuits of the proposed dual-band coupled-line coupler (operating at 1 and 3 GHz) for a: (a) -3-dB coupler, (b) -10-dB coupler, and (c) -20-dB coupler.

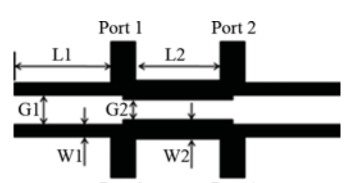

Fig. 7. Typical layout of the proposed dual-band coupler.

TABLE I
Dimensions of the Two Prototype Couplers (Unit: Millimeters)

Coupler	L1	L2	W1	W2	G1	G2
0.9/1.8 GHz	44.5	37.5	0.3	4	0.8	1
2.4/5.8 GHz	13.25	12	0.75	3.26	0.52	0.36

are $Z_{0e1} = Z_{0e2} = 185.9\ \Omega$ and $Z_{0o1} = Z_{0o2} = 26.9\ \Omega$; for the -10-dB coupler design, $Z_{0e1} = Z_{0e2} = 100.2\ \Omega$ and $Z_{0o1} = Z_{0o2} = 49.9\ \Omega$; and for the -20-dB coupler design,

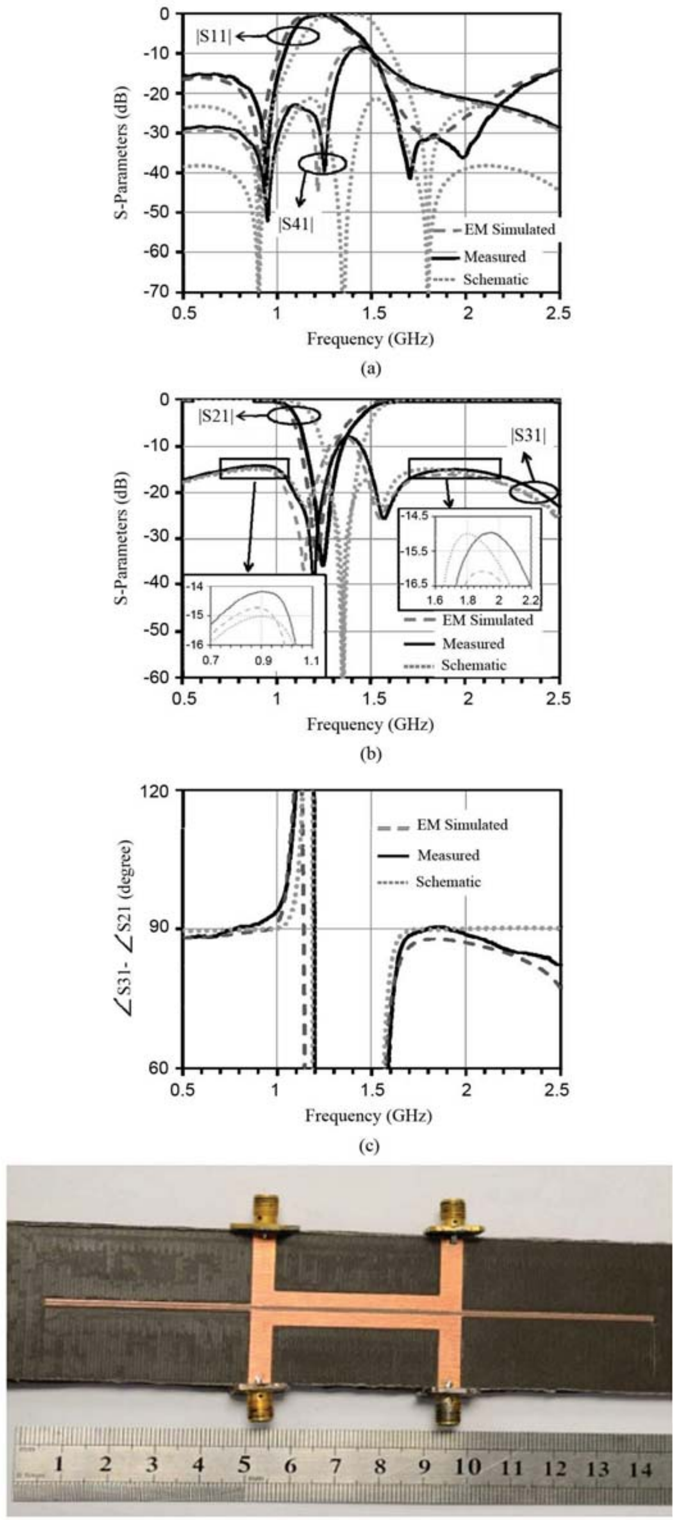

Fig. 8. EM simulated, schematic circuit, and measured results of the −15-dB prototype coupler operating at 0.9/1.8 GHz. (a) Magnitude of $S11$ and $S41$. (b) Magnitude of $S21$ and $S31$. (c) Phase difference between the two output ports. (d) Photograph of the prototype coupler on a double-sided PCB board.

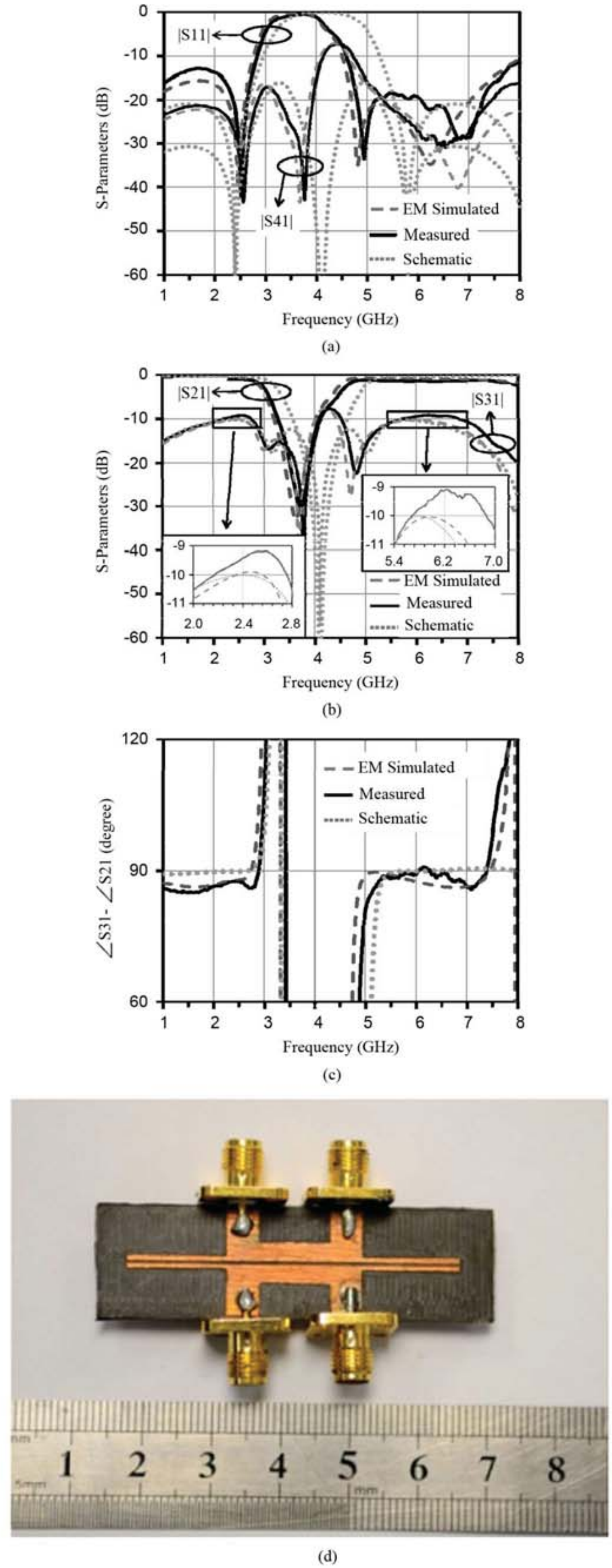

Fig. 9. EM simulated, schematic circuit, and measured results of the −10-dB coupler operating at 2.4/5.8 GHz. (a) Magnitude of $S11$ and $S41$. (b) Magnitude of $S21$ and $S31$. (c) Phase difference between the two output ports. (d) Photograph of the prototype coupler.

$Z_{0e1} = Z_{0e2} = 78.7\ \Omega$ and $Z_{0o1} = Z_{0o2} = 63.6\ \Omega$. Obviously, the phase difference between the two output ports remains nearly constant in a wideband range. The fractional bandwidths can be calculated under the conditions that $|S_{31}| = \Delta \pm 0.5$ dB, $|S_{11}| \leq -15$ dB, $|S_{41}| \leq -15$ dB, and $\angle S_{31} - \angle S_{21} = 90 \pm 1^\circ$, where Δ is the designated coupling coefficient. For the -3-dB coupler, the fractional bandwidths are about 54% and 18% at the two designated frequencies, respectively. For the -10-dB coupler, the fractional bandwidths are about 41% and 13.7%, respectively. For the -20-dB coupler, the fractional bandwidths are about 39% and 13%, respectively. It can be observed that the fractional bandwidths can be as wide as more than 13% at the second operating frequency even with a small coupling coefficient.

For verification purposes, two prototype couplers were designed, fabricated using a double-sided Duroid substrate with dielectric constant of 2.33 and thickness of 1.575 mm, and tested with Agilent E5071A. A representative layout of the prototype couplers is illustrated in Fig. 7. The first prototype was designed for the coupling coefficient of -15 dB. The two operating frequencies are 0.9 and 1.8 GHz. The second prototype is a -10-dB coupler operating at 2.4 and 5.8 GHz. The dimensions of the two prototype couplers are given in Table I. All the EM simulations were done by IE3D [17].

Fig. 8 shows the frequency responses of the -15-dB prototype coupler operating at 0.9/1.8 GHz. Due to the poor manufacturing quality of the in-house prototyping facility, the measured operating frequencies slightly shift to about 0.95/1.9 GHz and the coupling coefficient is a little bit larger than the designed value. The bandwidths at the two operating frequencies, in accordance with that $|S_{11}| \leq -15$ dB, $|S_{41}| \leq -15$ dB, $|S_{31}| = -14.5 \pm 0.5$ dB, and -15 ± 0.5 dB at the lower and higher operating frequencies, respectively, and $\angle S_{31} - \angle S_{21} = 90 \pm 5^\circ$ are 28.4% and 15.8%, respectively. As seen from Fig. 8(c), the phase difference between the two output ports remains almost constant in a wide frequency range.

Similar performance for the -10-dB prototype coupler operating at 2.4 and 5.8 GHz is shown in Fig. 9. The bandwidths at the two operating frequencies with respect to $|S_{11}| \leq -15$ dB, $|S_{41}| \leq -15$ dB, $|S_{31}| \leq -9.5 \pm 0.5$ dB, and $\angle S_{31} - \angle S_{21} = 90 \pm 5^\circ$, 22%, and 19.8%, respectively.

It should be mentioned that the EM simulated responses do not perfectly match to those of the ideal schematic circuit models at the higher frequency band due to the unequal even- and odd-mode velocities in microstrip coupled lines and dispersion effect of the T-junction discontinuous. A better way to reduce this effect is to use TEM transmission lines.

IV. Conclusion

In this paper, a novel planar dual-band coupled-line coupler has been proposed. The coupler can provide an arbitrary coupling coefficient at dual frequency bands with wider bandwidths as compared to its branch-line coupler counterpart. The coupler configuration is simple and only consists of three pairs of $\lambda/4$ coupled lines at the middle frequency of the two designated dual operating frequencies. The mathematical design formula is developed, which provides a straightforward analytic design procedure. Two prototype dual-band couplers with different coupling coefficients and frequency ratios have been designed by following the proposed design procedure and using a commercial EM simulator, fabricated and measured. Good correlation between the measured results and those of the designed verifies the circuit principle and the theoretic design formula.

References

[1] K.-P. Yang and K.-L. Wong, "Dual-band circularly-polarized square microstrip antenna," *IEEE Trans. Antennas Propag.*, vol. 49, no. 3, pp. 377–382, Mar. 2001.

[2] Y. Ding and K. K. Leung, "Dual-band circularly polarized dual-slot antenna with a dielectric cover," *IEEE Trans. Antennas Propag.*, vol. 57, no. 12, pp. 3757–3764, Dec. 2009.

[3] L.-C. Tsai and C.-W. Hsue, "Dual-band bandpass filters using equal-length coupled-serial-shunted lines and Z-transform technique," *IEEE Trans. Microw. Theory Tech.*, vol. 52, no. 4, pp. 1111–1117, Apr. 2004.

[4] S. Luo, L. Zhu, and S. Sun, "A dual-band ring-resonator bandpass filter based on two pairs of degenerate modes," *IEEE Trans. Microw. Theory Tech.*, vol. 58, no. 12, pp. 3427–3432, Dec. 2010.

[5] K.-K. M. Cheng and C. Law, "A novel approach to the design and implementation of dual-band power divider," *IEEE Trans. Microw. Theory Tech.*, vol. 56, no. 2, pp. 487–492, Feb. 2008.

[6] Y. Wu, Y. Liu, and Q. Xue, "An analytical approach for a novel coupled-line dual-band Wilkinson power divider," *IEEE Trans. Microw. Theory Tech.*, vol. 59, no. 2, pp. 286–294, Feb. 2011.

[7] I.-H. Lin, C. Caloz, and T. Itoh, "A branch-line coupler with two arbitrary operating frequencies using left-handed transmission lines," in *IEEE MTT-S Int. Microw. Symp. Dig.*, Jun. 2003, vol. 1, pp. 325–328.

[8] K.-K. M. Cheng and F.-L. Wong, "A novel approach to the design and implementation of dual-band compact planar 90° branch-line coupler," *IEEE Trans. Microw. Theory Tech.*, vol. 52, no. 11, pp. 2458–2463, Nov. 2004.

[9] H. Zhang and K. J. Chen, "A stub tapped branch-line coupler for dual-band operations," *IEEE Microw. Wireless Compon. Lett.*, vol. 17, no. 2, pp. 106–108, Feb. 2007.

[10] M.-J. Park, "Dual-band, unequal length branch-line coupler with center-tapped stubs," *IEEE Microw. Wireless Compon. Lett.*, vol. 19, no. 10, Oct. 2009.

[11] M.-J. Park and B. Lee, "Dual-band, cross coupled branch line coupler," *IEEE Microw. Wireless Compon. Lett.*, vol. 15, no. 10, pp. 6y55–6y57, Oct. 2005.

[12] H. Kim, B. Lee, and M.-J. Park, "Dual-band branch-line coupler with port extensions," *IEEE Trans. Microw. Theory Tech.*, vol. 58, no. 3, pp. 651–655, Mar. 2010.

[13] C.-L. Hsu, J.-T. Kuo, and C.-W. Chang, "Miniaturized dual-band hybrid couplers with arbitrary power division ratios," *IEEE Trans. Microw. Theory Tech.*, vol. 57, no. 1, pp. 149–156, Jan. 2009.

[14] C.-L. Hsu, "Dual-band branch line coupler with large power division ratios," in *Proc. Asia–Pacific Microw. Conf.*, Dec. 2009, pp. 1–4.

[15] L. K. Yeung, "A compact dual-band 90° coupler with coupled-line sections," *IEEE Trans. Microw. Theory Tech.*, vol. 59, no. 9, pp. 2227–2232, Sep. 2011.

[16] K. S. Ang Leong, Y. C. Leong, and C. H. Lee, "Multisection impedance-transforming coupled-line baluns," *IEEE Trans. Microw. Theory Tech.*, vol. 51, no. 2, pp. 536–541, Feb. 2003.

[17] IE3D Simulator. Zeland Softw. Inc., Fremont, CA, 1997.

Xi Wang was born in Chongqing, China, in 1984. He received the B.Eng. and M.Eng. degrees from the University of Electronic Science and Technology of China, Chengdu, China, in 2006 and 2009, respectively, and is currently working toward the Ph.D. degree at Shanghai Jiao Tong University, Shanghai, China.

From 2009 to 2010, he was with the Center for Microwave and RF Technologies, Shanghai Jiao Tong University. Since December 2010, he has been with the Department of Electronic Engineering, The Chinese University of Hong Kong, Shatin, Hong Kong, as a Research Assistant. His current research interests include passive RF and microwave circuits and filters for wireless applications.

Wen-Yan Yin (M'99–SM'01) received the M.Sc. degree in electromagnetic fields and microwave techniques from Xidian University, Xi'an, China, in 1989, and the Ph.D. degree in electrical engineering from Xi'an Jiao Tong University, Xi'an, China, in 1994.

From 1993 to 1996, he was an Associate Professor with the Department of Electronic Engineering, Northwestern Polytechnic University, Xi'an, China. From 1996 to 1998, he was a Research Fellow with the Department of Electrical Engineering, Duisburg University, Duisburg, Germany, granted by the Alexander von Humboldt-Stiftung, Bonn, Germany. Since December 1998, he has been with Department of Electrical Engineering, National University of Singapore (NUS), Singapore, as a Research Fellow. In March 2002, he joined the Temasek Laboratories, NUS, as a Research Scientist and a Project Leader. Since April 2005, he has been a Professor with the School of Electronic Information and Electrical Engineering, Shanghai Jiao Tong University, Shanghai, China. In January 2009, he joined the National State Key Laboratory of Modern Optical Instrumentation, Zhejiang University, Hangzhou, China, as a "Qiu Shi" Chair Professor. He has authored or coauthored over 190 international journal papers, one international book, and 17 book chapters. His main research interests include passive and active RF and millimeter-wave device and circuit modeling, ultra-wideband interconnects and signal integrity, nanoelectronics, electromagnetic compatibility (EMC) and electromagnetic protection, and computational multiphysics and applications.

Dr. Yin is an IEEE EMC Society Distinguished Lecturer from 2011 to 2012. He was the recipient of the Best Paper Award of the 2008 Asia–Pacific Symposium on Electromagnetic Compatibility and the 19th International Zurich Symposium, Singapore.

Ke-Li Wu (M'90–SM'96–F'11) received the B.S. and M.Eng. degrees from the Nanjing University of Science and Technology, Nanjing, China, in 1982 and 1985, respectively, and the Ph.D. degree from Laval University, Quebec, QC, Canada, in 1989. From 1989 to 1993, he was with the Communications Research Laboratory, McMaster University, as a Research Engineer and a Group Manager. In March 1993, he joined the Corporate R&D Division, COM DEV International, where he was a Principal Member of Technical Staff. Since October 1999, he has been with The Chinese University of Hong Kong, Hong Kong, where he is a Professor and the Director of the Radiofrequency Radiation Research Laboratory (R3L). He has authored or coauthored numerous publications in the areas of electromagnetic (EM) modeling and microwave and antenna engineering. His current research interests include PEEC and DPEC electromagnetic modeling of high-speed circuits, RF and microwave passive circuits and systems, synthesis theory and practices of microwave filters, antennas for wireless terminals, low-temperature co-fired ceramic (LTCC)-based multichip modules (MCMs), and RF identification (RFID) technologies.

Dr. Wu is a member of IEEE MTT-8 Subcommittee (Filters and Passive Components). He has served as a Technical Program Committee (TPC) member for many international conferences including the IEEE Microwave Theory and Techniques Society (IEEE MTT-S) International Microwave Symposium (IMS). He was an associate editor for the IEEE TRANSACTIONS ON MICROWAVE THEORY AND TECHNIQUES (2006–2009). He was the recipient of the 1998 COM DEV Achievement Award for the development of exact EM design software of microwave filters and multiplexers and the 2008 Asia–Pacific Microwave Conference Prize.